



# Morphological, molecular and toxinological analyses of *Alexandrium affine* (Dinophyceae) from marine coastal waters of Buenos Aires Province (Argentina)

JONÁS ADRIÁN TARDIVO KUBIS <sup>1</sup>, FRANCISCO RODRÍGUEZ <sup>2</sup>, ARACELI E. ROSSIGNOLI <sup>3</sup>, PILAR RIOBÓ <sup>4</sup>, DELFINA AGUIAR JUÁREZ <sup>1</sup>,  
EUGENIA ALICIA SAR <sup>1</sup> AND INÉS SUNESEN <sup>1</sup>

<sup>1</sup>División Ficología Dr. Sebastián Gurrera, FCNyM, UNLP, Paseo del Bosque s/n, 1900, La Plata, Argentina. CONICET

<sup>2</sup>Instituto Español de Oceanografía (IEO-CSIC), Subida a Radio Faro 50, 36390, Vigo, Spain

<sup>3</sup>Procesos Oceanográficos Costeiros, Centro de Investigações Mariñas (CIMA), Pedras de Corón s/n, 36620, Vilanova de Arousa, Spain

<sup>4</sup>Instituto de Investigaciones Marinas, CSIC, Eduardo Cabello, 6, 36208 Vigo, Spain

## ABSTRACT

In the framework of a monitoring program of harmful microalgae from the marine coastal waters of Buenos Aires Province to mitigate the impacts of harmful algal blooms on the aquaculture and marine life and to protect human health, a strain of *Alexandrium affine* (LPCc012) was isolated. *Alexandrium affine* is a worldwide distributed species reported as harmful algal bloom-forming, with toxin- and non-toxin-producing strains. Field and cultured materials from Buenos Aires Province were examined using light and scanning electron microscopy, morphologically and genetically (LSU rDNA partial sequencing) characterized, and compared with material from different regions worldwide. Toxin analyses using ultra-performance liquid chromatography with fluorescence detection and liquid chromatography-mass spectrometry methods failed to detect any paralytic or lipophilic shellfish toxins. This is the first record of *A. affine* from Argentina.

## ARTICLE HISTORY

Received 29 December 2022

Accepted 07 June 2023

Published Online 20 July 2023

## KEYWORDS

Cell morphology; First report from Argentina; Molecular characterization; Phylogeny; Toxin assessment

## INTRODUCTION

The genus *Alexandrium* Halim has a cosmopolitan distribution in coastal waters and includes about thirty-three accepted species (Guiry & Guiry 2022). Several of these are potentially toxic and responsible for paralytic shellfish poisoning (PSP) outbreaks (Anderson *et al.* 2012; Branco *et al.* 2020). Additionally, *Alexandrium* displays a unique toxin diversity because, in addition to different paralytic shellfish toxins (PST), some species can also produce lipophilic toxins such as spirolides (SPXs), gymnodimines (GYMs), goniodomines (GDs) and uncharacterized bioactive extracellular compounds (BECs) (Anderson *et al.* 2012; Suikkanen *et al.* 2013; Van de Waal *et al.* 2015; Long *et al.* 2021). The sanitary risk of these compounds is drastically different for public health; ingestion of PST-contaminated shellfish can cause human poisonings (and in extreme cases, fatalities), while human intoxications by SPXs, GYMs or GDs have never been recorded (Krock *et al.* 2018; Sunesen *et al.* 2021).

To date, eight species of *Alexandrium* have been documented for the Argentine Sea: *A. acatenella* (Whedon & Kofoid) Balech (now interpreted as representing *A. catenella*), *A. catenella* (Whedon & Kofoid) Balech, *A. fraterculus* (Balech) Balech, *A. kutnerae* (Balech) Balech, *A. tamarense* (M. Lebour) Balech and '*A. tropicale* Balech', *nom. inval.*, were recorded by Balech (1995). Subsequently, *A. minutum* Halim was recorded by Fabro *et al.* (2017) and *A. ostenfeldii* (Paulsen) Balech & Tangen by Almandoz *et al.* (2014), Fabro *et al.* (2017) and Guinder *et al.* (2018).

Balech (1995) indicated members of the *A. tamarense* complex as the only PST producer *Alexandrium* species in Argentinian marine waters. The molecular analyses (LSU rDNA partial sequencing, D1–D3 regions) given by Penna *et al.* (2008), Fabro *et al.* (2017), Guinder *et al.* (2018), Blossom *et al.* (2019) and Tardivo Kubis *et al.* (2023) showed that strains ascribed to the *A. tamarense* complex in Argentina always belong to *A. catenella* (John *et al.* 2014). In turn, *A. catenella* isolated from Argentinian waters shows variable toxin profiles. These can be dominated by N-sulfocarbamoyl-11-hydrosulfate toxins (C1,2) and secondarily by gonyautoxins 1,4 (GTX1,4) (Carreto *et al.* 2001; Montoya *et al.* 2010; Krock *et al.* 2015; Guinder *et al.* 2018; Tardivo Kubis *et al.* 2023), or with GTX1,4 as main component and a minor presence of C1,2 (Almandoz *et al.* 2019); or dominated by GTX2,3 and secondarily by GTX1,4 (Tardivo Kubis *et al.* 2023), similar to what as described by Varela *et al.* (2012) from Aysén, Chile.

Quantitative polymerase chain reaction (qPCR) analyses from net tow samples (NT) confirmed the association of *A. minutum* with PST in plankton samples, in which GTX1,4 was the main component (Fabro *et al.* 2017). These results agree with those by Oshima *et al.* (1989) for Australian strains and by Liu *et al.* (2022) for Chinese and Malaysian strains.

The *Alexandrium ostenfeldii* complex from the Beagle Channel was associated with SPXs in cell cultures: 13-desmethyl spirolide C (SPX-1) and 20-methyl spirolide G (20-Me-SPX-G) (Almandoz *et al.* 2014). Subsequently, Fabro *et al.* (2017) confirmed the presence of *A. ostenfeldii* by qPCR assay from NT samples and its relationship with the detection of

SPXs, SPX-1 and 20-Me-SPX-G. According to Anderson *et al.* (2012) and Suikkanen *et al.* (2013) this species produces either saxitoxin (STX) and its analogues, or SPXs, but rarely both. Nevertheless, *A. ostenfeldii* isolated by Guinder *et al.* (2018) from El Rincón (Northern Patagonian shelf in the Argentine Sea), produced PSTs dominated by GTX2,3 followed by C1,2 and, additionally, SPXs dominated by SPX-1 followed by a novel spirolide (SPX-M) and other five minor SPXs.

In the framework of a phytoplankton and biotoxin monitoring program implemented since 2008 in marine coastal waters of the Buenos Aires Province, a new *Alexandrium* sp. strain (LPCc012) was isolated. The objectives of this monitoring program are to mitigate the impacts of harmful algal blooms (HABs) on the aquaculture and marine life, and to protect human health (Sunesen *et al.* 2014; Tardivo Kubis *et al.* 2019). To that goal, the isolation and characterization of potentially toxic species, with special attention to new findings in the area, are essential to track their presence and relationship with regional HAB events.

The aim of this study is to provide an integrated morphological, molecular (LSU rDNA sequencing and phylogeny), and toxinological analysis of *Alexandrium* sp. strain LPCc012 and to compare the results obtained with those in the literature.

## MATERIAL AND METHODS

### Isolation and culture of strain

A clonal strain of *Alexandrium* sp. (LPCc012) was established from a surface seawater sample collected with 30 µm mesh net hauls in marine coastal waters of Mar Azul (Buenos Aires Province, Argentina), near the shoreline.

Single cells were isolated by micropipette using a Zeiss Axiovert 40 CFL inverted microscope with phase contrast and differential interference contrast (DIC) (Zeiss Microimaging, Goettingen, Germany). Individual cells were washed several times in local filtered seawater until free of contaminants and transferred into six-well tissue culture plates containing 10 ml of natural seawater enriched with Guillard's *f/2* medium without silicates (Sigma-Aldrich, Saint Louis, USA). Cells were incubated at 16°C and salinity of 30, under the irradiance of 100–125 µmol photons m<sup>-2</sup> s<sup>-1</sup> supplied by cool-white fluorescent tubes, in a 12:12 light:dark regime, in a growth chamber (SEMEDIC I-290F, SEMEDIC SRL, CABA, Argentina). Once established, the culture was seeded in 40 ml (final volume) using 100-ml flasks, and maintained in the conditions described above.

### Microscopy

For light microscopy (LM) analyses, live cells of the strain LPCc012 were observed using a Leica DMLA microscope (Leica Microsystems, Wetzlar, Germany) equipped with DIC and with a Zeiss Axiovert 40 CFL microscope (with phase contrast and DIC) (Carl Zeiss Microscopy GmbH, Jena, Germany). Photographs were taken with a Leica DFC420c digital camera and a Canon PowerShot G10 (Canon Cameras USA, Melville, New York, USA).

For scanning electron microscopy (SEM) analyses, samples were fixed in 4% formaldehyde (final concentration). Sample suspension (1 ml) was collected on nylon (polyamide) filter membranes (13 mm diameter, 0.45 µm pore-size, Sartolon polyamide Sartorius Stedim Biotech, Goettingen, Germany) in a filter funnel and rinsed in distilled water. Filters were dehydrated in an ethanol series of 30%, 50%, 70%, 90%, 95% and 100% with 10 min at each concentration, and then critical-point dried (BalTec, model CPD-30, Balzers, Liechtenstein). Filters were mounted on aluminum stubs, sputter-coated with gold-palladium using a Cressington 108 (Cressington Scientific Instruments, Watford, UK) and subsequently observed with a NTS SUPRA 40 FE-SEM (Carl Zeiss Microscopy). Micrographs were analysed using Image J software (Schneider *et al.* 2012).

Field material and SEM stubs were deposited in the Herbarium of the División Ficología (LPC), Facultad de Ciencias Naturales y Museo, Universidad Nacional de La Plata, under collection numbers LPC11403, LPC11411 and LPC11471.

### DNA extraction, amplification and sequencing

An aliquot (1.5 ml) of a culture in late exponential growth phase was concentrated by centrifugation, washed in two drops of milli-Q water, placed in 200-µl microtubes, cold shocked in liquid nitrogen and kept at -20°C until further analysis. DNA extraction used Chelex® chelating resin (Bio-Rad, Hercules, California, USA), following Richlen & Barber (2005). Final extracts were kept at -20°C before PCR analyses. The D1–D3 domains of the LSU rDNA were amplified using the pairs of primers D1R/D2C (5'-ACCCGCTGAATTTAAGCATA-3'/5'-ACGAACGATTTGCACGTCAG-3', Lenaers *et al.* 1989; Litaker *et al.* 2003).

The amplification reaction mixtures (20 µl) were performed using Horse-Power™ Taq DNA Polymerase MasterMix (Canvax, Spain) following the manufacturer's instructions. The DNA was amplified in a Mastercycler EP5345 (Eppendorf AG, New York, USA). PCR reactions were checked by agarose gel electrophoresis (1% TAE, 80 V) and GelRed™ nucleic acid gel staining (Biotium, Hayward, California, USA). PCR products were purified with ExoSAP-IT™ (U+SB Corporation, Cleveland, Ohio, USA) and purified DNA was sequenced using the Big Dye Terminator v3.1 Reaction Cycle Sequencing kit (Applied Biosystems, Foster City, California, USA) and migrated in an AB 3130 sequencer (Applied Biosystems) at the CACTI sequencing facilities (University of Vigo, Spain).

### Phylogenetic analyses

The partial LSU rRNA gene sequences obtained were inspected and aligned using MEGA X software (Kumar *et al.* 2018). *Lingulodinium polyedra* (F. Stein) J.D. Dodge was used to root the tree. The original LSU rDNA alignment (including gaps) consisted of 730 bp. The best evolutionary models for maximum likelihood (ML) phylogenetic analyses were estimated using the model selection tool in MEGA X software, and Tamura-Nei model (Tamura & Nei 1993) was selected. Initial tree(s) for the heuristic search were obtained

automatically by applying Neighbor-Join and BioNJ algorithms to a matrix of pairwise distances estimated using the Maximum Composite Likelihood (MCL) approach, and then selecting the topology with superior log likelihood value. A discrete Gamma distribution was used to model evolutionary rate differences among sites [5 categories (+G, parameter = 0.7003)]. The tree is drawn to scale, with branch lengths measured in the number of substitutions per site. This analysis involved 63 nucleotide sequences. All positions with less than 95% site coverage were eliminated, i.e. fewer than 5% alignment gaps, missing data and ambiguous bases were allowed at any position (partial deletion option). There was a total of 559 positions in the final dataset.

Additionally, a Bayesian inference (BI) analysis was carried out by sampling across the entire GTR model space using Mr. Bayes v3.2 (Huelsenbeck & Ronquist 2001). The program parameters were statefreqpr, dirichlet (1,1,1,1); nst, mixed; and rates, gamma. Phylogenetic analyses involved two parallel analyses, each with four chains. Starting trees for each chain were selected randomly using the default values for the Mr. Bayes program. The number of generations used in these analyses was 1,000,000. Posterior probabilities were calculated from every 100th tree sampled after log-likelihood stabilization (burn-in phase). All final split frequencies were <0.02. The two methods rendered similar topologies. The LSU rDNA phylogenetic tree represented BI results, with bootstrap values and posterior probabilities from ML and BI analyses, respectively.

Net mean *p*-distances between phylogenetic clades were calculated using MEGA X. No corrections for multiple substitutions at the same site, substitution rate biases (e.g. differences in the transitional and transversional rates), or differences in evolutionary rates among sites were considered (Nei & Kumar 2000).

### Toxin extraction and analysis

Lugol-fixed aliquots of 5 ml of strain LPCc012, were collected from two cultures to determine cell density by LM using a Sedgewick-Rafter chamber. Cultures were harvested for toxin analysis during the mid-exponential growth phase, filtered through 25 mm diameter glass fiber filters (Whatman) and placed in Eppendorf tubes.

### PARALYTIC SHELLFISH TOXINS

Extraction of PSTs was performed by adding 750  $\mu$ l 0.05M acetic acid into the tube containing 477,092 cells and frozen at  $-20^{\circ}\text{C}$  until further use. Just before analysis the sample was sonicated for 1 min at 50 watts (4710 Series Ultrasonic Homogenizer, 40 footswitch) and centrifuged at  $5,200\times g$  and  $10^{\circ}\text{C}$  for 10 min. The supernatant was collected in a clean Eppendorf tube. The extraction was repeated with another 750  $\mu$ l of 0.05M acetic acid. Both supernatants were combined (final volume 1,500  $\mu$ l) and then filtered through 0.22- $\mu$ m PTFE syringe filters prior to HPLC analyses. To verify the presence of toxins C1, C2, C3, C4, GTX5 and GTX6, equal volumes of the sample and 0.4 N HCl were boiled for 15 min to hydrolyse the sulfonic group of the

sulfocarbamoil to give GTX2, GTX3, GTX1, GTX4, STX and neosaxitoxin (NeoSTX), respectively.

The characterization of PSTs in the *Alexandrium* sp. strain was performed by ultra-performance liquid chromatography with fluorescence detection and post-column oxidation (UPLC-FLD-PCOX) method (Rourke *et al.* 2008) with slight modifications. A Waters Acquity ultra performance liquid chromatography (UPLC) system (Waters Corporation) was used and separation of toxins was performed onto a Waters XBridge<sup>®</sup> Shield RP, 4.6 x 150 mm, 3.5  $\mu$ m column maintained at  $35^{\circ}\text{C}$ . Mobile phase A was composed of 11 mM heptane sulfonic acid sodium salt in a 5.5 mM phosphoric acid aqueous solution adjusted to pH 7.1 with 0.5 M ammonium hydroxide. Mobile phase B consisted of 88.5% 11 mM heptane sulfonic acid sodium salt in a 16.5 mM phosphoric acid aqueous solution adjusted to pH 7.1 with 0.5 M ammonium hydroxide and 11.5% acetonitrile. The mobile phases were filtered through a 0.2- $\mu$ m-pore, 47 mm diameter nylon membrane filter (Whatman) before use. The mobile phases mixture was run at a flow rate of 1 ml  $\text{min}^{-1}$  starting at 95% A 5% B and held for 13 min, changing to 100% B on minute 13.01 until minute 20, and returning to initial conditions at minute 20.1 until minute 26. An equilibration time of 5 min was allowed prior to the next injection. The eluate from the column was mixed continuously with 7 mM periodic acid in 50 mM potassium phosphate buffer (pH = 9.0) at a rate of 0.4 ml  $\text{min}^{-1}$  and was heated at  $65^{\circ}\text{C}$  by passage through a coil of Teflon tubing (0.25 mm i.d., 8 m long). It was then mixed with 0.5 M acetic acid at 0.4 ml  $\text{min}^{-1}$  and pumped by a two-pump Waters Reagent Manager into the fluorescence detector, which was operated at an excitation wavelength of 330 nm, recording emission at 390 nm. The injection volumes were 20 and 40  $\mu$ l for non-hydrolysed and hydrolysed samples, respectively. A total of 15 PST analogues were screened: C1, C2, C3, C4, GTX1, GTX2, GTX3, GTX4, GTX5, GTX6, decarbamoyl gonyautoxins (dcGTX2, dcGTX3), decarbamoyl saxitoxin (dcSTX), NeoSTX and STX. Limits of detection (LODs) of PST analogues were calculated based on the standard deviation of the response (Sx/y) of the calibration curve and the slope at levels approximating the LOD according to the formula  $\text{LOD} = 3.3(\text{Sx/y})$ , and they were expressed in fmol  $\text{cell}^{-1}$ . The differential toxicities of STX analogs are also reported as STX equivalents (STX eq) based on conversion factor as follows: STX = 1, dcSTX = 1, NeoSTX = 1, GTX1 = 1, GTX2 = 0.4, GTX3 = 0.6, GTX4 = 0.7, dcGTX2 = 0.2 and dcGTX3 = 0.4 (European Food Safety Authority EFSA 2009) and they were expressed in fmol STX eq  $\text{cell}^{-1}$  (Table 1). Certified Reference PSTs standards for STX, NeoSTX, dcSTX, (GTX)-1,2,3,4 and (dcGTX)-2,3 were purchased from the National Research Council Canada (NRCC-CRMs).

### LIPHILIC TOXINS

For lipophilic toxin extraction, 1 ml of MeOH was added to a tube containing 292,500 cells and sonicated for 1 min (Branson 450 cell disruptor). The obtained extract was centrifuged at  $4,700\times g$  for 10 min (Heraeus Multifuge X3 FR, Thermo Scientific) and filtered through 0.22  $\mu$ m syringe filters (Membrane Solutions, Jasco Spain, Madrid, Spain), and then analysed.

**Table 1.** Limits of detection of the standard analogues of PSP toxins used in this work expressed in terms of concentration (fmol cell<sup>-1</sup>) and toxicity (fmol STX eq cell<sup>-1</sup>).

Toxins	fmol cell <sup>-1</sup>	fmol STX eq cell <sup>-1</sup>
STX	1.22	1.22
dcSTX	1.72	1.72
NeoSTX	2.70	2.70
GTX3	0.40	0.24
GTX2	0.48	0.19
dcGTX3	0.18	0.07
dcGTX2	0.89	0.18
GTX4	2.29	1.6
GTX1	2.53	2.53

The analyses have been carried out on an Exion LC AD™ System (SCIEX, Framingham, Massachusetts, USA) coupled to a Qtrap 6500+ mass spectrometer (SCIEX) through an IonDrive TurboV interface in electrospray mode. A total of 31 azaspiracids (AZAs), nine SPXs, three brevetoxins (PbTXs), four pinnatotoxins (PnTXs), 13 GYMs, four GDs, okadaic acid (OA), two dinophysistoxins (DTXs) and two yessotoxins (YTXs) were screened according to Rossignoli *et al.* (2021), with slight modifications. Briefly, the toxins were separated using a Gemini NX column 50 mm (length) × 2 mm (id), 3 µm (particle size) from Phenomenex (Torrance, California, USA). Mobile phase A was water and B MeCN 90%, both containing 6.7 mM NH<sub>4</sub>OH (pH = 11). The gradient started with 22% B, was maintained for 0.5 min, followed by a linear increment to reach 95% B at minute 3.85, and maintaining this composition until minute 6.25. The composition was then returned linearly to the initial one in 0.5 min and maintained 2 min before the next injection. The flow rate was 0.4 µl min<sup>-1</sup>, the injection volume was 2 µl and the column temperature was 40°C.

The mass spectrometer parameters were optimized by direct infusion using toxin standards, when available, and were set to: ion source gas 1, 75 (arbitrary units); ion source gas 2, 75 (arbitrary units); ion spray voltage, 5,000 (positive) and -4,500 (negative); capillary temperature, 600°C; curtain gas, 30; collision gas, medium; declustering potential (DEP), entrance potential (EP) and collision cell exit potential (CXP) were ± 80 V, 15 V and ± 11 V, respectively.

The transitions with collision energies used for screening of each toxin and the limits of detection (LODs), calculated only for those toxins for which certified reference materials are available, are shown in Table 2.

## RESULTS

### Morphological analysis

The determination of *Alexandrium affine* became evident after morphological and molecular analyses as reported below. Strain label: LPCc012, collected 9 February 2017 at Mar Azul (MAZ)

(37°20.63'S, 57°1.52'W); GenBank accession number: MZ838950. Field material labels: LPC 11403, Villa Gesell (VG) (37°16.80'S, 56°58.95'W), collected 25 February 2015; LPC 11411, VG, collected 30 March 2015; LPC 11471, Santa Teresita (ST) (36°32.50'S, 56°41.18'W), collected 2 February 2017.

### *Alexandrium affine* (H. Inoue & Fukuyo) Balech Figs 1–11

REFERENCES: Fukuyo *et al.* (1985, p. 30, figs 1E, 3A–3C, 24–29; as *Protogonyaulax affinis*); Hallegraeff *et al.* (1991, p. 584, figs 43–50); Balech (1995, p. 55, pl. 13, figs 20–36).

MORPHOLOGY: Chain-forming species, 2–16 cells long (Figs 1, 2), the cell chains becoming shorter as the culture ages (Figs 3, 4). Cells were small to large, 29–60 µm long and 26–51 µm wide (n = 100), with many golden-brown, elongated chloroplasts (Figs 3, 4), and a U-shaped nucleus (Fig. 4, n). The theca was subpentagonal (in ventral and dorsal views), smooth, with many scattered two-sized pores (Figs 7, 8, s = small, l = large). The epitheca was convex-conical, with subtle shoulders, and slightly longer than the hypotheca (Figs 3, 4, 7). The pore plate (Po) was subrectangular, with convex left margin and straight right margin perpendicular to the almost straight dorsal margin and to the slightly concave ventral margin (Figs 9, 10). The Po had an oval, ventral foramen (f) occluded by a conopeum with a short callus in ventral position (Fig. 5) and a large, circular, anterior connecting pore (acp) above the foramen in dorsal position (Figs 5, 10 arrowed). The first apical plate (1') was directly connected with Po, and was asymmetrically rhomboidal, with a ventral pore (v) in the right margin at about middle height (Fig. 7). Plate 6' was pentagonal, wide and high, with concave left margin (Fig. 7). The cingulum was descendent by about one circular width, deeply excavated and bordered by narrow lists (Figs 7, 8). The sulcus was deep, bordered by lists, with the left one wider than the right (Figs 7, 8, arrow). The sulcal posterior plate (Sp) was trapezoidal, with a circular posterior connecting pore (pcp; Figs 6, 8, 11) linked to the right margin by a channel (ch; Figs 6, 11 arrow).

DISTRIBUTION: *Alexandrium affine* was found in marine coastal waters of Santa Teresita, Villa Gesell and Mar Azul (Buenos Aires Province), and this is the first record of the species from Argentina. Previously, *A. affine* was found in the following locations: Sarom Lake, connected with Okhotsk Sea, and Mutsu Bay and Seto Inland Sea, Japan (Fukuyo *et al.* 1985); Ría de Vigo, Spain (Fraga *et al.* 1988); South-eastern Australian water, Bell Bay, Northern Tasmania (Hallegraeff *et al.* 1991); Carquín Bay, Huacho Bay and La Arenilla Beach, Callao, Perú (Vera *et al.* 1999); Sebatu and Pulau Aman in the Straits of Malacca s/d, Malaysia (Usup *et al.* 2002); Bay of Concarneau, Brittany, France (Guillou *et al.* 2002); Bahía Concepción (26°33'–26°53'N, 111°42'–112°56'W) connected with the Gulf of California (Band-Schmidt *et al.* 2003); Lisbon Bay, Portugal (Moita *et al.* 2003); Ha Long Bay, Tonkin Gulf, North Vietnam (Nguyen-Ngoc 2004); South-east China Sea (Wang *et al.* 2006); South China Sea, East China Sea and Yellow Sea, China (Gu *et al.* 2013); Kadan Island, southern Myanmar coast (Myat & Koike 2013); Honda Bay, Palawan, Philippines (Subong *et al.* 2017); Jinhae-Masan Bay, Korea (Kim *et al.* 2017); Punta del Este, Uruguay (Méndez *et al.* 2020); southern Mediterranean lagoon, Mellah, Algeria (Draredja *et al.* 2020).

### Molecular analysis

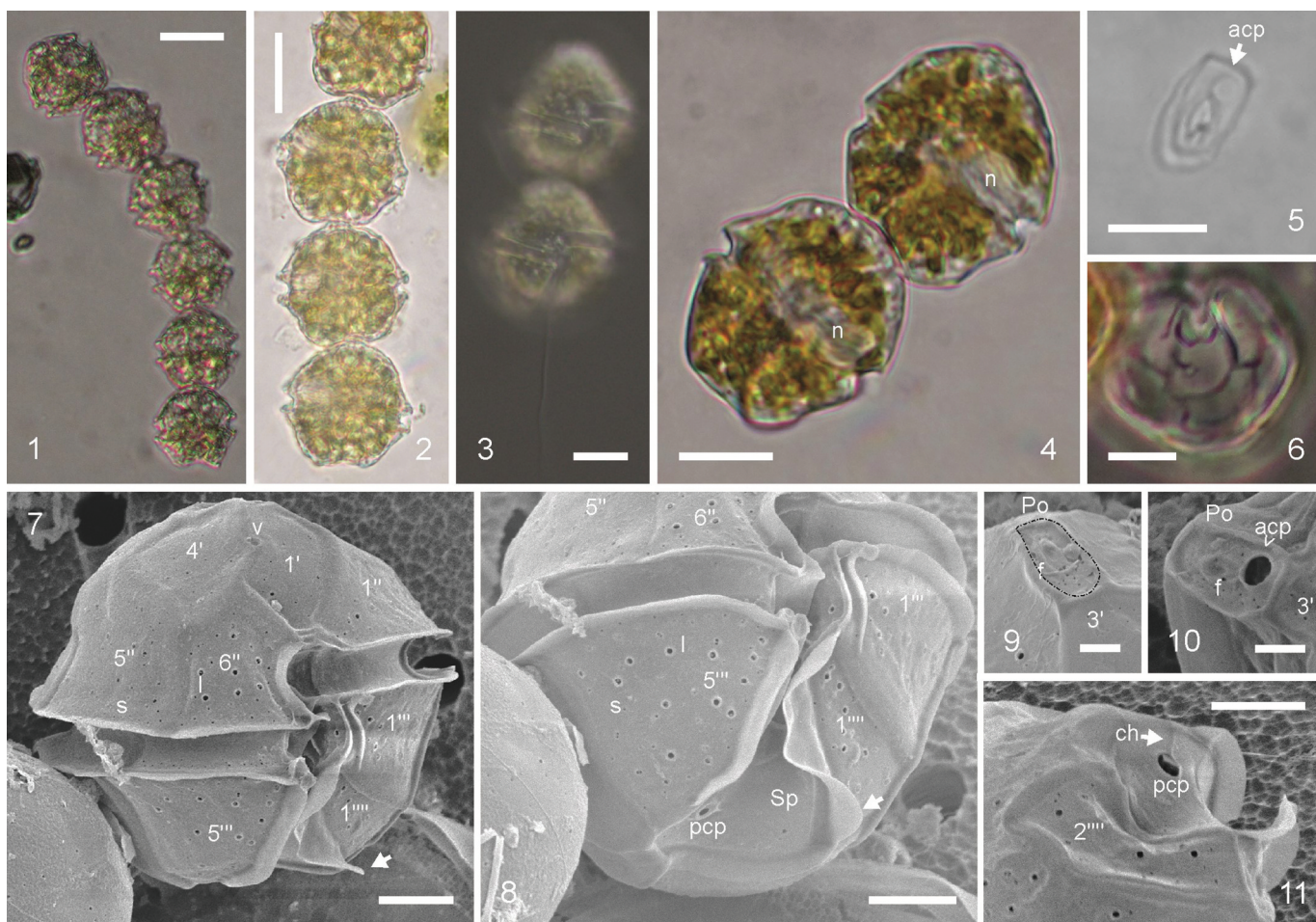
An alignment comprising sequences from 63 taxa, including 16 species of *Alexandrium*, three of *Centrodinium* and the studied

**Table 2.** MS/MS fragmentation conditions for lipophilic toxin screening. ESI, electrospray ionization mode; Q1, m/z ratio in the first quadrupole; Q3, m/z ratio in the third quadrupole; CE (v), collision energy; LOD, limit of detection (fg cell<sup>-1</sup>).

Toxin	ESI	Q1	Q3	CE (v)	LOD, fg cell <sup>-1</sup>
AZA 1	POS	842.5	824.5	40	7.69
AZA 6,40	POS	842.5	824.5	40	–
AZA 2	POS	856.5	838.5	40	7.69
AZA 2 phosphate	POS	936.5	918.5	40	–
AZA 3	POS	828.5	810.4	40	7.69
AZA 43,58	POS	828.5	810.4	40	–
AZA 4,56	POS	844.5	826.5	40	–
AZA 5	POS	844.5	826.3	40	–
AZA 7,8,9,10,36	POS	858.5	840.5	40	–
AZA 11	POS	872.5	854.4	40	–
AZA 11 phosphate	POS	952.5	818.5	40	–
AZA 12	POS	872.5	854.5	40	–
AZA 33	POS	716.5	698.4	40	–
AZA 34,39	POS	816.5	798.4	40	–
AZA 35,38	POS	830.5	812.5	40	–
AZA 37	POS	846.5	828.5	40	–
AZA 41	POS	854.5	846.5	40	–
AZA 42, 54, methyl AZA 2	POS	870.5	852.5	40	–
AZA 55	POS	868.5	362.2	50	–
AZA 57	POS	884.5	866.5	40	–
SPX-1	POS	692.4	164.3	60	0.17
SPX G	POS	692.4	164.3	60	–
SPX A	POS	692.4	150.3	60	–
SPX B	POS	694.4	150.3	60	–
13,19 diDesMethyl SPX C	POS	678.5	164.3	60	0.03
20-Me-SPX-G	POS	706.5	164.3	60	0.94
SPX C, SPX C2	POS	706.5	164.3	60	–
13 desmethyl SPX D	POS	694.4	164.3	60	–
PbTX 2	POS	895.4	319.2	40	–
PbTX 3	POS	897.5	725.4	20	–
PbTX 9	POS	899.5	157.2	50	–
PnTX A	POS	712.5	164.3	70	–
PnTX E	POS	784.5	164.3	70	–
PnTX F	POS	766.5	164.3	70	–
PnTX G	POS	694.5	458.3	55	0.34
GYM A	POS	508.3	392.2	55	1.03
GYM B, C, D	POS	524.3	136.2	60	–
GYM E, F	POS	526.3	136.2	60	–
GYM G, H	POS	556.3	136.2	60	–
12 methyl GYM A, GYM J	POS	522.3	136.2	60	–
12 methyl GYM B, C	POS	538.3	136.2	60	–
16 desmethyl GYM D	POS	510.3	136.2	60	–
Goniodomine A, B	POS	786.5	733.5	35	–
34 desmethyl GD A, 9 desmethyl GD A	POS	772.5	719.5	35	–
OA	NEG	803.5	255.2	–62	2.56
DTX 1	NEG	817.5	255.2	–60	7.69
DTX 2	NEG	803.5	255.2	–62	7.69
YTX	NEG	570.4	467.4	–42	18.80
HomoYTX	NEG	577.4	474.4	–42	20.51

*A. affine* strain LPCc012, was used in the present work to infer phylogenetic relationships. The topological structures of the trees obtained using ML and BI were similar and only the BI tree is shown (Fig. 12). The results placed LPCc012 in the *A. affine* clade with strong support. No differences in the amplified region were observed between isolates from distinct geographical origins. The

branching pattern placed *A. affine* as a sister group to the *Centrodinium* clade, and in secondary relation with *A. tamarense* and *A. fraterculus* species groups (Fig. 12). Accordingly, low net mean distances ( $p$ ) of these closest groups to *A. affine* were found (0.05 for the *Centrodinium* clade, 0.103 for the *A. tamarense* group and 0.143 for the *A. fraterculus* group).



**Figs 1–11.** *Alexandrium affine*, LM and SEM.

**Figs 1, 2.** Chains of six and four cells. Field material, LPC 11403 VG 25-02-2015 (Fig. 1) and LPC 11471 ST 02-02-2017 (Fig. 2). Scale bars = 20  $\mu$ m.

**Figs 3, 4.** Chain of two cells. The U-shaped nuclei (n) are visible in Fig. 4. Cultured material, LPCc012 MAZ 09-02-2017 (Genbank accession MZ838950). Scale bars = 10  $\mu$ m.

**Fig. 5.** Detail of the pore plate (Po). Note the anterior connecting pore (acp, arrowed) above the foramen. Same material as in Figs 3, 4. Scale bar = 5  $\mu$ m.

**Fig. 6.** Cell in antapical view showing detail of the posterior sulcal plate (Sp). Note the posterior connecting pore (pcp) linked to the right margin by a channel. Same material as in Figs 3, 4. Scale bar = 10  $\mu$ m.

**Fig. 7.** Whole cell. The left wider list is indicated by an arrow. s, small pores; l, large pores. Note plate 1' with ventral pore (vp) on the suture with 4'. Field material, SEM, LPC 11411 VG 30-03-2015. Scale bar = 5  $\mu$ m.

**Fig. 8.** Detail of Fig. 7, showing the left wider list (arrow). s, small pores; l, large pores. Note the posterior sulcal plate (Sp) showing the posterior connecting pore (pcp). Field material, same as in Fig. 7. Scale bar = 5  $\mu$ m.

**Figs 9, 10.** Apical pore plate (Po), almost rectangular. Po is shown delimited by a dotted line in Fig. 9. Note the ventral foramen (f) and absence of anterior connecting pore in

**Fig. 10.** Note the ventral foramen (f) occluded by a conopeum and the anterior connecting pore (acp) in dorsal position. Field material, same as in Fig. 7. Scale bars = 2  $\mu$ m.

**Fig. 11.** Detail of the Sp showing the pcp linked to the right margin by a channel (ch). Field material, same as in Fig. 7. Scale bars = 5  $\mu$ m.

## Toxin analysis

Carbamate toxins reported in *A. affine* to date (STX, NeoSTX, GTX1, GTX2, GTX3 and GTX4) have not been detected in the strain LPCc012 analysed in this work. Neither decarbamoyl STX analogues (dcSTX, dcGTX2 and dcGTX3) nor N-sulfo-carbamoyl (C1, C2, C3, C4, GTX5 and GTX6) were detected in both non-hydrolysed and hydrolysed extracts. In addition, none of the toxins belonging to the lipophilic group (SPXs, GYMs, GDs, PbTXs, PnTXs, AZAs, OA, DTXs, YTXs) were detected (all data <LOD).

## DISCUSSION

*Alexandrium affine* is a chain-forming species, with a ventral pore as other members of the *A. fraterculus* group (Balech 1995). It can be distinguished by the morphology of the pore plate (Po), which is subrectangular, with a large, circular, anterior connecting pore

(acp) above the foramen (f) in dorsal position (Fukuyo *et al.* 1985; Steidinger & Tangen 1997; Myat & Koike 2013). The comparison between specimens of *A. affine* in this study and those described in the literature is summarized in Table 3.

*Alexandrium affine* from Buenos Aires forms chains (2–16 cells long) as described in the protologue by Fukuyo *et al.* (1985), by Vera *et al.* (1999; chains of 2–32 cells), Hallegraeff *et al.* (1991; 2–4 cells), Band-Schmidt *et al.* (2003; 2–8, sometimes 16 cells) and Nguyen-Ngoc (2004; 4–12 cells). Cell size range in strains and field material in this study was similar to that described by Fukuyo *et al.* (1985) and Band-Schmidt *et al.* (2003), but larger than reported in other works (Table 3). The specimens analysed in this study agree well with those in the literature (Table 3) regarding cell shape, shape and position of the plates, form and position of the pore (and the acp on the Po plate), form of plate 1' and presence of vp, form of plate Sp and position of the pcp,

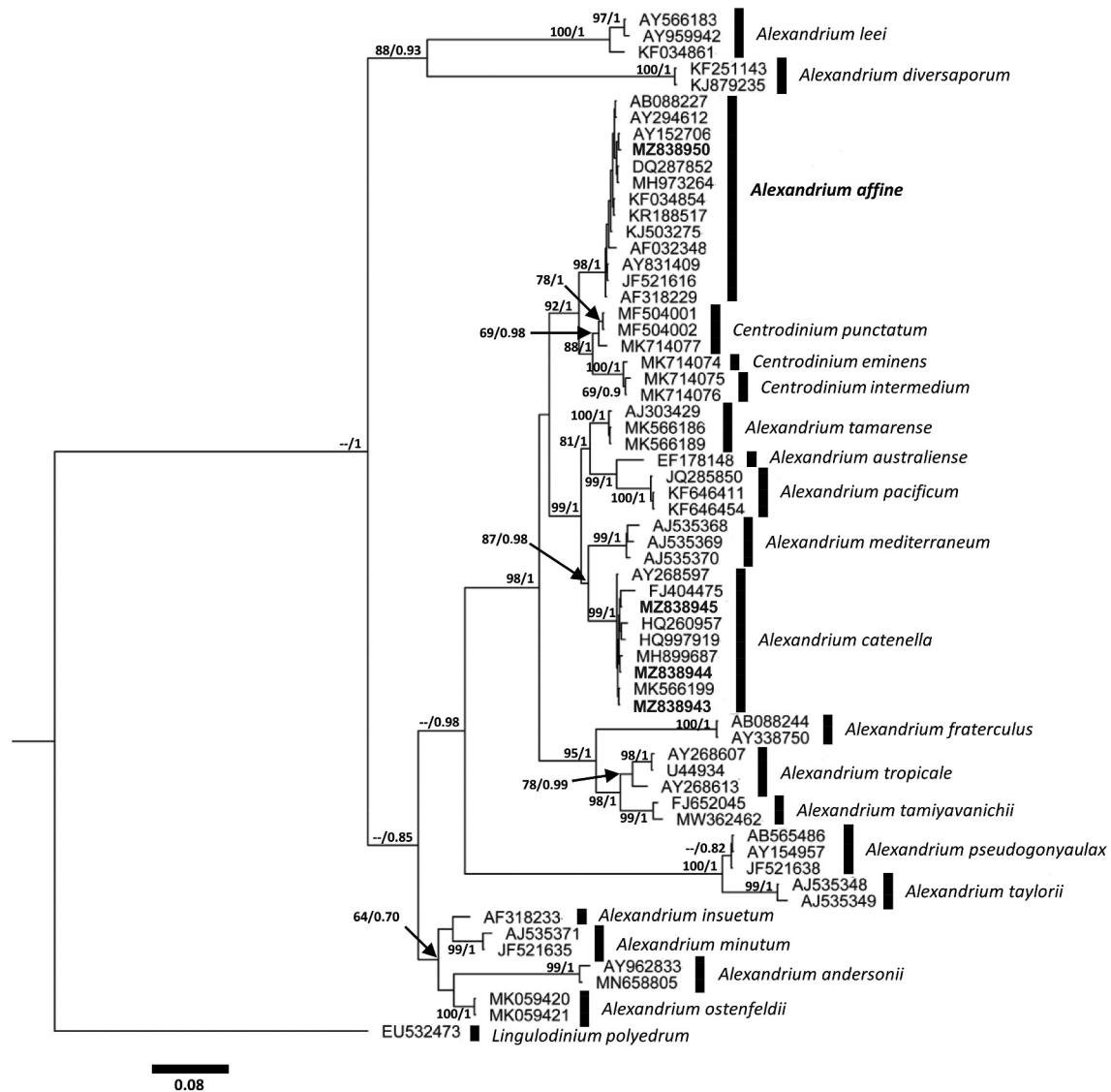


**Fig. 12.** Phylogenetic tree of the D1–D3 LSU rDNA obtained by BI model showing the *Alexandrium affine* strain (in bold) from Buenos Aires coastal waters and its relationships with other strains of *Alexandrium* and *Centrodinium*. The tree includes sequences of *Alexandrium catenella* (MZ838943, Los Pocitos; MZ838944, San Blas Bay and MZ838945, Ria Jabali), from Buenos Aires coastal waters (Tardivo Kubis et al. 2023). Numbers next to branches are bootstrap percentages ( $n = 1,000$ ) and posterior probabilities ( $n = 1,000,000$ ) after ML and BI analyses, respectively. Values lower than 60%/0.60 or not representative in one of the analyses are not shown or replaced with hyphens, respectively.

and form of plate 6". Additionally, studied specimens exhibited two distinctively different size classes of pores on the thecal surface, consistent with those described by Fukuyo et al. (1985) and those shown by Hallegraef et al. (1991, figs 43, 44, 46), Usup et al. (2002, figs 2B–2D), Nguyen-Ngoc (2004, figs 4, 5, 7) and Kim et al. (2017, figs 1D–1L). This feature was also detected in *A. leei* Balech, not described by Balech (1995) but shown by Usup et al. (2002, figs 3B–3D), and in '*A. camurascutulum* Mackenzie & Todd', *nom. inval.*, not described in the protologue but shown in Mackenzie & Todd (2002, figs 1–12). Moreover, the presence of two size classes of thecal pores on the plates was subsequently described for *A. diversaporum* Sh. Murray et al. by Murray et al. (2014, figs 2A–2G, 3A–3B, 4A–4D, 5A–5G, 6A–6F). A comprehensive morphological comparison between species with two size classes of thecal pores was summarized by Murray et al. (2014, table 1).

Despite the fact that *A. affine* is among the easiest *Alexandrium* species to differentiate using morphological features, its identity was also confirmed by LSU rDNA sequencing, and distinguished from other species such as those belonging to the former *A. tamarensis* species complex (including *A. catenella*, *A. mediterraneum* U. John, *A. tamarensis*, *A. pacificum* Litaker and *A. australiense* Sh. Murray) (John et al. 2014), the *A. fraterculus* group (including *A. affine*, *A. tamiyavanichii* Balech and *A. fraterculus*) (Gu et al. 2013; Murray et al. 2014; Fabro et al. 2017) and the surprisingly close members of the genus *Centrodinium* Kofoid (Li et al. 2019; Tillmann et al. 2021).

Phylogenetic analyses of the genus *Alexandrium* including *A. affine*, depict different topologies regarding this species depending on the marker regions, sequence alignments and approach used (Touzet et al. 2008). Some of these studies shown the *A. affine* clade closer to the *A. tamarensis* species

**Table 3.** Comparison of *Alexandrium affine* from Buenos Aires coastal waters and from different places worldwide based on morphology and production of PST.

References	Cell size in $\mu\text{m}$	1'	Po/acp position	Sp	From	PST
This study	29–60 $\mu\text{m}$ long 26–51 $\mu\text{m}$ wide	asymmetric rhomboidal, with a vp in the right margin at about half height	subrectangular, with circular, large, dorsal acp	subtrapezoidal with a pcp linked to the right margin by a channel	Mar Azul, Buenos Aires Province, Argentina	negative
Fukuyo <i>et al.</i> (1985)	24–67 $\mu\text{m}$ long 24–71 $\mu\text{m}$ wide	asymmetric rhomboidal*, with a vp in the anterior third of the suture between 1' and 4'	subrectangular, with a circular dorsal acp	subtrapezoidal* with a pcp linked to the right margin by a channel*	Sarom Lake, Japan	nd
Hallegraeff <i>et al.</i> (1991)	25–32 $\mu\text{m}$ in diameter	asymmetric rhomboidal*, with a vp in the anterior third of the suture between 1' and 4'	subrectangular, with a circular dorsal right acp	subtrapezoidal* with a pcp linked to the right margin by a channel	Bell Bay, sediments, northern Tasmania	negative
Balech (1995)	26–44 $\mu\text{m}$ long 24–44 $\mu\text{m}$ wide	asymmetric rhomboidal*, with a vp (in the right margin*) at about half height	bullet-shaped, with a large dorsal acp	subpentagonal*, with a pcp, linked to the right margin by a channel	Bay of Jinhae, Korea	negative
Vera <i>et al.</i> (1999)	29 $\mu\text{m}$ long 39 $\mu\text{m}$ wide	asymmetric rhomboidal*, with a vp (in the right margin*)	bullet-shaped*, with a dorsal acp	subpentagonal with a pcp, linked to the right margin by a channel*	Huacho Bay, Carquín Bay and La Arenilla beach, Perú	doubtful, GTX3 and GTX2*
Band-Schmidt <i>et al.</i> (2003)	29–66 $\mu\text{m}$ long 23–65 $\mu\text{m}$ wide	asymmetric rhomboidal*, with a vp in the right margin	subrectangular, with a large round anterior acp	subtrapezoidal* with pcp	Concepción Bay, Gulf of California, México	negative
Nguyen-Ngoc (2004)	30–40 $\mu\text{m}$ in diameter	1' and the position of the vp varied widely in morphology	bullet-shaped* with or without acp	subrectangular* with or without pcp, linked to the right margin by a channel*	Ha Long Bay, Tonkin Gulf, North Vietnam	toxic and not toxic, NeoSTX, STX and GTX1–4,
Gu <i>et al.</i> (2013)	33–43 $\mu\text{m}$ long 30–40 $\mu\text{m}$ wide	asymmetric rhomboidal*, with a small vp at the suture between plates 1' and 4'	nd	trapezoidal, with a pcp near the middle of the right margin	South China Sea, East China Sea and Yellow Sea, China	negative
Myat & Koike (2013)	28–44 $\mu\text{m}$ long 23–43 $\mu\text{m}$ wide	long rhomboidal, with a small vp in the middle of the right margin	narrow and long with acp directly above the apical pore	longer than wide, with a rounded pcp located near the middle of the right margin, linked with a small channel	Kadan Island, Southern Myanmar coast	nd
Subong <i>et al.</i> (2017)	25 $\mu\text{m}$ long 22 $\mu\text{m}$ wide	asymmetric rhomboidal* with a vp in the right margin	acp on top of the plate	nd	Honda Bay, Palawan, Philippines	STX and NeoSTX GTX1,4
Kim <i>et al.</i> (2017)	30 $\mu\text{m}$ long 24 $\mu\text{m}$ wide	rhomboidal, with a vp in the right margin	bullet-shaped, with a large acp at the dorsal one-third of plate	pentagonal with or without pcp	Jinhae-Masan Bay, Korea	nd
Méndez <i>et al.</i> (2020)	22–29 $\mu\text{m}$ long 24 $\mu\text{m}$ in diameter	asymmetric rhomboidal*, with a vp (in the right margin*) at about middle height	long, bullet-shaped, with a large acp at the dorsal part of the plate	subtrapezoidal* with a pcp, linked to the right margin by a channel	Punta del Este, Uruguay	doubtful, GTX3*

1', first apical plate; Po, pore plate; vp, ventral pore; Sp, sulcal posterior plate; PST, paralytic shellfish toxins; acp, anterior connecting pore; pcp, posterior connecting pore; nd, no data; \* data evaluated from the corresponding quoted paper; GTX1–4, gonyautoxins 1–4, STX, saxitoxin; NeoSTX, neosaxitoxin.

complex (Guillou *et al.* 2002; Hansen *et al.* 2003; Kim *et al.* 2004; Onda *et al.* 2013; John *et al.* 2014; Subong *et al.* 2017; Xu *et al.* 2021), others exhibit tighter relationships with the *A. fraterculus* group (Montresor *et al.* 2004; Gu *et al.* 2013; Murray *et al.* 2014; Almandoz *et al.* 2019; Benico & Azanza 2021) or even with species of the fusiform, armoured dinoflagellate genus *Centrodinium* (Li *et al.* 2019; Gómez & Artigas *et al.* 2019; Mertens *et al.* 2020; Tillmann *et al.* 2021).

In this study, both the ML and BI analyses grouped *A. affine* with *Centrodinium* species with high bootstrap percentage and posterior probability support (92/1 respectively). These results are in line with those reported by Gómez & Artigas *et al.* (2019) using D1–D3 LSU rDNA sequence data and by Li *et al.* (2019) and Tillmann *et al.* (2021) using concatenated rDNA sequences data.

Previous toxicological studies have demonstrated that *A. affine* is a potential PST producer. Some strains do not produce any PSTs, like those analysed by Hallegraeff *et al.* (1991) from Tasmania, Band-Schmidt *et al.* (2003) from Bahía Concepción, Gulf of California, Mexico, and Wang *et al.* (2006) from South-east China Sea. Instead, other strains proved to be toxic, like those analysed by Nguyen-Ngoc (2004) from Ha Long Bay, Tonkin Gulf, Vietnam and by Subong *et al.* (2017) from Honda Bay, Palawan, Philippines, which contained STX, NeoSTX and GTX1,4. Previously, toxin analyses in South America were not conclusive about the relationship between GTX2 and GTX3 with *A. affine* blooms. Vera *et al.* (1999) detected GTX2 and GTX3 in acid extracts of *Argopecten purpuratus* exposed to a bloom of *A. affine* in Carquín Bay, Huacho Bay and La

Arenilla beach, central coast of Perú. Méndez *et al.* (2020) detected a minor chromatographic peak whose retention time could match GTX3 from mussels exposed to a bloom of *A. affine* in coastal waters of Punta del Este, Uruguay. In contrast, the LPCc012 Argentinian strain from this study did not produce any toxic compounds, either PSTs or lipophilic toxins otherwise detected in some *Alexandrium* species (SPXs, GYMs and GDs), nor any other toxins targeted by our analytical method (such as PbTXs, PnTXs, AZAs, OA, DTXs, YTXs).






## ACKNOWLEDGEMENTS

We thank two anonymous reviewers for helping us to improve the original manuscript. This study was partially supported by grants from the Universidad Nacional de La Plata (11/N863), Consejo Nacional de Investigaciones Científicas y Técnica (PIP 11220200101920CO), with the contribution of the Dirección Provincial de Pesca, Ministerio de Desarrollo Agrario, Prov. Buenos Aires, and by the projects CCVIEO and DIANAS (CTM2017-86066-R) from the Instituto Español de Oceanografía and the TOXEMER project PGIDIT-CIMA 21/01 from Consellería do Mar (Xunta de Galicia), with additional funds of the Axencia Galega de Innovación (agreement GAIN-IEO).

## DISCLOSURE STATEMENT

No potential conflict of interest was reported by the authors.

## ORCID

Jonás Adrián Tardivo Kubis  <http://orcid.org/0000-0002-3172-4955>  
 Francisco Rodríguez  <http://orcid.org/0000-0002-6918-4771>  
 Araceli E. Rossignoli  <http://orcid.org/0000-0002-6052-9067>  
 Pilar Riobó  <http://orcid.org/0000-0002-1921-6229>  
 Delfina Aguiar Juárez  <http://orcid.org/0000-0002-8733-5107>  
 Eugenia Alicia Sar  <http://orcid.org/0000-0003-2912-4528>  
 Inés Sunesen  <http://orcid.org/0000-0003-3219-456X>

## REFERENCES

- Almandoz G.O., Montoya N.G., Hernando M.P., Benavides H.R., Carignan M.O. & Ferrario M.E. 2014. Toxic strains of the *Alexandrium ostenfeldii* complex in southern South America (Beagle Channel, Argentina). *Harmful Algae* 37: 100–109. DOI: [10.1016/j.hal.2014.05.011](https://doi.org/10.1016/j.hal.2014.05.011).
- Almandoz G.O., Cefarelli A.O., Diodato S., Montoya N., Benavides H.R., Carignan M., Hernando M., Fabro E., Metfies K., Lundholm N. *et al.* 2019. Harmful phytoplankton in the Beagle Channel (South America) as a potential threat to aquaculture activities. *Marine Pollution Bulletin* 145: 105–117. DOI: [10.1016/j.marpolbul.2019.05.026](https://doi.org/10.1016/j.marpolbul.2019.05.026).
- Anderson D.M., Alpermann T.J., Cembella A.D., Collos Y., Masseret E. & Montresor M. 2012. The globally distributed genus *Alexandrium*: multifaceted roles in marine ecosystems and impacts on human health. *Harmful Algae* 14: 10–35. DOI: [10.1016/j.hal.2011.10.012](https://doi.org/10.1016/j.hal.2011.10.012).
- Balech E. 1995. *The genus Alexandrium Halim (Dinoflagellata)*. Sherkin Island Marine Station Publication, Sherkin Island Co. Cork, Ireland. 151 pp.
- Band-Schmidt C.J., Lechuga-Devéze C.H., Kulis D.M. & Anderson D.M. 2003. Culture studies of *Alexandrium affine* (Dinophyceae), a non-toxic cyst forming dinoflagellate from Bahía Concepción, Gulf of California. *Botanica Marina* 46: 44–54. DOI: [10.1515/BOT.2003.007](https://doi.org/10.1515/BOT.2003.007).
- Benico G. & Azanza R. 2021. Characterization of *Alexandrium tamutum* (Dinophyceae) isolated from Philippine waters, with the rare detection of paralytic shellfish toxin. *Philippine Journal of Systematic Biology* 15: 1–13. DOI: [10.26757/pjsb2021a15009](https://doi.org/10.26757/pjsb2021a15009).
- Blossom H.E., Markussen B., Daugbjerg N., Krock B., Norlin A. & Hansen P.J. 2019. The cost of toxicity in microalgae: direct evidence from the dinoflagellate *Alexandrium*. *Frontiers in Microbiology* 10: Article 1065. DOI: [10.3389/fmicb.2019.01065](https://doi.org/10.3389/fmicb.2019.01065).
- Branco S., Oliveira M.M.M., Salgueiro F., Vilar M.C.P., Azevedo S.M.F. O. & Menezes M. 2020. Morphology and molecular phylogeny of a new PST-producing dinoflagellate species: *Alexandrium fragae* sp. nov. (Gonyaulacales, Dinophyceae). *Harmful Algae* 95: Article 101793. DOI: [10.1016/j.hal.2020.101793](https://doi.org/10.1016/j.hal.2020.101793).
- Carreto J.L., Carignan M.O. & Montoya N.G. 2001. Comparative studies on mycosporine-like amino acids, paralytic shellfish toxins and pigment profiles of the toxic dinoflagellate *Alexandrium tamarense*, *A. catenella* and *A. minutum*. *Marine Ecology Progress Series* 223: 49–60. DOI: [10.3354/meps223049](https://doi.org/10.3354/meps223049).
- Draredja M.A., Frihi H., Boualleg C., Abadie E. & Laabir M. 2020. Distribution of dinoflagellate cyst assemblages in recent sediments from a southern Mediterranean lagoon (Mellah, Algeria) with emphasis on toxic species. *Environmental Science and Pollution Research* 27: 25173–25185. DOI: [10.1007/s11356-020-08830-0](https://doi.org/10.1007/s11356-020-08830-0).
- EFSA 2009. Scientific opinion of the panel on contaminants in the food chain on a request from the European Commission on marine biotoxins in shellfish: saxitoxin group (question No EFSA-Q-2006-065E). *EFSA Journal* 1019: 1–76.
- Fabro E., Almandoz G.O., Ferrario M.E., John U., Tillmann U., Toebe K., Krock B. & Cembella A. 2017. Morphological, molecular and toxin analysis of field populations of *Alexandrium* genus from the Argentine Sea. *Journal of Phycology* 53: 1206–1222. DOI: [10.1111/jpy.12574](https://doi.org/10.1111/jpy.12574).
- Fraga S., Anderson D.M., Bravo I., Reguera B., Steidinger K. & Yentsch C.M. 1988. Influence of upwelling relaxation on dinoflagellates and shellfish toxicity in Ria de Vigo, Spain. *Estuarine, Coastal and Shelf Science* 27: 349–361. DOI: [10.1016/0272-7714\(88\)90093-5](https://doi.org/10.1016/0272-7714(88)90093-5).
- Fukuyo Y., Yoshida K. & Inoue H. 1985. *Protogonyaulax* in Japanese coastal waters. In: *Toxic dinoflagellates* (Ed. by D.M. Anderson, A. W. White & D.G. Baden), pp 27–32. Elsevier, Amsterdam, Netherlands.
- Gómez F. & Artigas L.F. 2019. Redefinition of the dinoflagellate genus *Alexandrium* based on *Centrodinium*: reinstatement of *Gessnerium* and *Protogonyaulax*, and *Episemicolon* gen. nov. (Gonyaulacales, Dinophyceae). *Journal of Marine Biology* 2019: Article 1284104. DOI: [10.1155/2019/1284104](https://doi.org/10.1155/2019/1284104).
- Gu H., Zeng N., Liu T., Yang W., Müller A. & Krock B. 2013. Morphology, toxicity, and phylogeny of *Alexandrium* (Dinophyceae) species along the coast of China. *Harmful Algae* 27: 68–81. DOI: [10.1016/j.hal.2013.05.008](https://doi.org/10.1016/j.hal.2013.05.008).
- Guillou L., Nézan E., Cueff V., Erard-Le Denn E., Cambon-Bonavita M.-A., Gentien P. & Barbier G. 2002. Genetic diversity and molecular detection of three toxic dinoflagellate genera (*Alexandrium*, *Dinophysis* and *Karenia*) from French coasts. *Protist* 153: 223–238. DOI: [10.1078/1434-4610-00100](https://doi.org/10.1078/1434-4610-00100).
- Guinder V.A., Tillmann U., Krock B., Delgado A.L., Krohn T., Garzón Cardona J.E., Metfies K., López Abbate C., Silva R. & Lara R. 2018. Plankton multiproxy analyses in the northern Patagonian shelf, Argentina: community structure, phycotoxins, and characterization of toxic *Alexandrium* strains. *Frontiers in Marine Science* 5: 75–95. DOI: [10.3389/fmars.2018.00394](https://doi.org/10.3389/fmars.2018.00394).
- Guiry M.D. & Guiry G.M. 2022. *AlgaeBase*. World-wide electronic publication, National University of Ireland, Galway. <https://www.algaebase.org>; searched on 27 June 2022.
- Hallegraeff G.M., Bolch C.J., Blackburn S.I. & Oshima Y. 1991. Species of the toxigenic dinoflagellate genus *Alexandrium* in southeastern Australian waters. *Botanica Marina* 34: 575–587. DOI: [10.1515/botm.1991.34.6.575](https://doi.org/10.1515/botm.1991.34.6.575).
- Hansen G., Daugbjerg N. & Franco J.M. 2003. Morphology, toxin composition and LSU rDNA phylogeny of *Alexandrium minutum* (Dinophyceae) from Denmark, with some morphological observations on other European strains. *Harmful Algae* 2: 317–335. DOI: [10.1016/S1568-9883\(03\)00060-X](https://doi.org/10.1016/S1568-9883(03)00060-X).
- Huelsenbeck J.P. & Ronquist F. 2001. MRBAYES: Bayesian inference of phylogenetic trees. *Bioinformatics* 17: 754–755. DOI: [10.1093/bioinformatics/17.8.754](https://doi.org/10.1093/bioinformatics/17.8.754).

- John U., Litaker R.W., Montresor M., Murray S., Brosnahan M.L. & Anderson D.M. 2014. Formal revision of the *Alexandrium tamarensis* species complex (Dinophyceae) taxonomy: the introduction of five species with emphasis on molecular-based (rDNA) classification. *Protist* 165: 779–804. DOI: [10.1016/j.protis.2014.10.001](https://doi.org/10.1016/j.protis.2014.10.001).
- Kim C.-J., Yoshihiko S., Aritsune U. & Kim C.-H. 2004. Molecular phylogenetic relationships within the genus *Alexandrium* (Dinophyceae) based on the nuclear-encoded SSU and LSU rDNA D1-D2 sequences. *Journal of the Korean Society of Oceanography* 39: 172–185.
- Kim E.S., Li Z., Oh S.J., Yoon Y.H. & Shin H.H. 2017. Morphological Identification of *Alexandrium* species (Dinophyceae) from Jinhae-Masan Bay, Korea. *Ocean Science Journal* 52: 427–437. DOI: [10.1007/s12601-017-0031-6](https://doi.org/10.1007/s12601-017-0031-6).
- Krock B., Borel C.M., Barrera F., Tillmann U., Fabro E., Almandoz G.O., Ferrario M., Garzón Cardona J.E., Koch B.P., Alonso C. *et al.* 2015. Analysis of the hydrographic conditions and cyst beds in the San Jorge Gulf, Argentina, that favor dinoflagellate population development including toxigenic species and their toxins. *Journal of Marine Systems* 148: 86–100. DOI: [10.1016/j.jmarsys.2015.01.006](https://doi.org/10.1016/j.jmarsys.2015.01.006).
- Krock B., Ferrario M.E., Akselman R. & Montoya N.G. 2018. Occurrence of marine biotoxins and shellfish poisoning events and their causative organisms in Argentine marine waters. *Oceanography* 31: 132–144. DOI: [10.5670/oceanog.2018.403](https://doi.org/10.5670/oceanog.2018.403).
- Kumar S., Stecher G., Li M., Knyaz C. & Tamura K. 2018. MEGA X: Molecular Evolutionary Genetics Analysis across computing platforms. *Molecular Biology and Evolution* 35: 1547–1549. DOI: [10.1093/molbev/msy096](https://doi.org/10.1093/molbev/msy096).
- Lenaers G., Maroteaux L., Michot B. & Herzog M. 1989. Dinoflagellates in evolution. A molecular phylogenetic analysis of large subunit ribosomal RNA. *Journal of Molecular Evolution* 29: 40–51. DOI: [10.1007/BF02106180](https://doi.org/10.1007/BF02106180).
- Li Z., Mertens K.N., Nézan E., Chomérat N., Bilién G., Iwataki M. & Shin H.H. 2019. Discovery of a new clade nested within the genus *Alexandrium* (Dinophyceae): morpho-molecular characterization of *Centrodinium punctatum* (Cleve) F.J.R. Taylor. *Protist* 170: 168–186. DOI: [10.1016/j.protis.2019.02.003](https://doi.org/10.1016/j.protis.2019.02.003).
- Litaker R.W., Vandarsea M.W., Kibler S.R., Tester P.A., Reece K.S., Stokes N.A., Steidinger K.A., Millie D.F., Bendis B.J. & Pigg R.J. 2003. Identification of *Pfiesteria piscicida* (Dinophyceae) and *Pfiesteria*-like organisms using internal transcribed spacer-specific PCR assays. *Journal of Phycology* 39: 754–761. DOI: [10.1111/j.0022-3646.2003.03906001\\_104.x](https://doi.org/10.1111/j.0022-3646.2003.03906001_104.x).
- Liu M., Krock B., Yu R., Leaw C.P., Lim P.T., Ding G., Wang N., Zheng J. & Gu H. 2022. Co-occurrence of *Alexandrium minutum* (Dinophyceae) ribotypes from the Chinese and Malaysian coastal waters and their toxin production. *Harmful Algae* 115: Article 102238. DOI: [10.1016/j.hal.2022.102238](https://doi.org/10.1016/j.hal.2022.102238).
- Long M., Krock B., Castrec J. & Tillmann U. 2021. Unknown extracellular and bioactive metabolites of the genus *Alexandrium*: a review of overlooked toxins. *Toxins* 13: Article 905. DOI: [10.3390/toxins13120905](https://doi.org/10.3390/toxins13120905).
- MacKenzie L. & Todd K. 2002. *Alexandrium camurascutulum* sp. nov. (Dinophyceae): a new dinoflagellate species from New Zealand. *Harmful Algae* 1: 295–300. DOI: [10.1016/S1568-9883\(02\)00045-8](https://doi.org/10.1016/S1568-9883(02)00045-8).
- Méndez S.M., Rodríguez F., Martínez A., Riobó P. & Vargas-Montero M. 2020. First report of *Alexandrium affine* in Uruguay: molecular, morphological and toxicological study of a bloom during summer 2017. In: *Harmful Algae 2018 – from ecosystems to socio ecosystems. Proceedings of the 18th International Conference on Harmful Algae, ISSHA, Nantes, France* (Ed. by P. Hess), pp 109–112.
- Mertens K.N., Adachi M., Anderson D.M., Band-Schmidt C.J., Bravo I., Brosnahan M.L., Bolch C.J.S., Calado A.J., Carbonell-Moore M.C., Chomérat N. *et al.* 2020. Morphological and phylogenetic data do not support the split of *Alexandrium* into four genera. *Harmful Algae* 28: Article 101902. DOI: [10.1016/j.hal.2020.101902](https://doi.org/10.1016/j.hal.2020.101902).
- Moita M.T., Oliveira P.B., Mendes J.C. & Palma A.S. 2003. Distribution of chlorophyll a and *Gymnodinium catenatum* associated with coastal upwelling plumes off central Portugal. *Acta Oecologica* 24: S125–S132. DOI: [10.1016/S1146-609X\(03\)00011-0](https://doi.org/10.1016/S1146-609X(03)00011-0).
- Montoya N.G., Fulco V.K., Carignan M.O. & Carreto J.I. 2010. Toxin variability in cultured and natural populations of *Alexandrium tamarensis* from southern South America-evidences of diversity and environmental regulation. *Toxicon* 56: 1408–1418. DOI: [10.1016/j.toxicon.2010.08.006](https://doi.org/10.1016/j.toxicon.2010.08.006).
- Montresor M., John U., Beran A. & Medlin L.K. 2004. *Alexandrium tamutum* sp. nov. (Dinophyceae): a new nontoxic species in the genus *Alexandrium*. *Journal of Phycology* 40: 398–411. DOI: [10.1111/j.1529-8817.2004.03060.x](https://doi.org/10.1111/j.1529-8817.2004.03060.x).
- Murray S.A., Hoppenrath M., Or R.J.S., Bolch C., John U., Diwan R., Yauwenas R., Harwood T., de Salas M., Neilan B. *et al.* 2014. *Alexandrium diversaporum* nov. sp., a new non-saxitoxin producing species: phylogeny, morphology and *sxtA* genes. *Harmful Algae* 31: 54–65. DOI: [10.1016/j.hal.2013.09.005](https://doi.org/10.1016/j.hal.2013.09.005).
- Myat S. & Koike K. 2013. A red tide off the Myanmar coast: morphological and genetic identification of the dinoflagellate composition. *Harmful Algae* 27: 149–158. DOI: [10.1016/j.hal.2013.05.010](https://doi.org/10.1016/j.hal.2013.05.010).
- Nei M. & Kumar S. 2000. *Molecular evolution and phylogenetics*. Oxford University Press, New York, USA. 333 pp.
- Nguyen-Ngoc L. 2004. An autecological study of the potentially toxic dinoflagellate *Alexandrium affine* isolated from Vietnamese waters. *Harmful Algae* 3: 117–129. DOI: [10.1016/S1568-9883\(03\)00062-3](https://doi.org/10.1016/S1568-9883(03)00062-3).
- Onda D.F.L., Benico G., Sulit A.F., Gaité P.L., Azanza R.V. & Lluisma A. O. 2013. Morphological and molecular characterization of some HAB-forming dinoflagellates from Philippine waters. *Philippine Science Letter* 6: 97–106.
- Oshima Y., Hirota M., Yasumoto T., Hallegraef G.M., Blackburn S.I. & Steffensen D.A. 1989. Production of paralytic shellfish toxins by the dinoflagellate *Alexandrium minutum* Halim from Australia. *Nippon Suisan Gakkaishi* 55: 925.
- Penna A., Fraga S., Masó M., Giacobbe M.G., Bravo I., Garcés E., Vila M., Bertozzini E., Andreoni F., Lugliè A. *et al.* 2008. Phylogenetic relationships among the Mediterranean *Alexandrium* (Dinophyceae) species based on sequences of 5.8S gene and Internal Transcript Spacers of the rRNA operon. *European Journal of Phycology* 43: 163–178. DOI: [10.1080/09670260701783730](https://doi.org/10.1080/09670260701783730).
- Richlen M.L. & Barber P.H. 2005. A technique for the rapid extraction of microalgal DNA from single live and preserved cells. *Molecular Ecology Notes* 5: 688–691. DOI: [10.1111/j.1471-8286.2005.01032.x](https://doi.org/10.1111/j.1471-8286.2005.01032.x).
- Rosignoli A.E., Mariño C., Martín H. & Blanco J. 2021. Development of a fast liquid chromatography coupled to mass spectrometry method (LC-MS/MS) to determine fourteen lipophilic shellfish toxins based on fused-core technology: in-house validation. *Marine Drugs* 19: Article 603. DOI: [10.3390/md19110603](https://doi.org/10.3390/md19110603).
- Rourke W.A., Murphy C.J., Pitcher G., van de Riet J.M., Burns B.G., Thomas K.M. & Quilliam M.A. 2008. Rapid postcolumn methodology for determination of paralytic shellfish toxins in shellfish tissue. *Journal of AOAC International* 91: 589–597.
- Schneider C.A., Rasband W.S. & Eliceiri K.W. 2012. NIH image to imageJ: 25 years of image analysis. *Nature Methods* 9: 671–675. DOI: [10.1038/nmeth.2089](https://doi.org/10.1038/nmeth.2089).
- Steidinger K. & Tangen K. 1997. Dinoflagellates. In: *Identifying marine phytoplankton* (Ed. by C.R. Tomas), pp 387–584. Acad. Press, Inc. San Diego, USA.
- Subong B.J.J., Benico G.A., Sulit A.K.L., Mendoza C.O., Cruz L.J., Azanza R.V. & Jimenez E.C. 2017. Toxicity and protein expression of *Alexandrium* species collected in the Philippine waters. *Philippine Journal of Science* 146: 425–436.
- Suikkanen S., Kremp A., Hautala H. & Krock B. 2013. Paralytic shellfish toxins or spiroclides? The role of environmental and genetic factors in toxin production of the *Alexandrium ostenfeldii* complex. *Harmful Algae* 26: 52–59. DOI: [10.1016/j.hal.2013.04.001](https://doi.org/10.1016/j.hal.2013.04.001).
- Sunesen I., Lavigne A.S., Goya A. & Sar E.A. 2014. Episodios de toxicidad en moluscos de aguas marinas costeras de la Provincia de Buenos Aires (Argentina) asociados a algas toxigenas (Marzo de 2008-Marzo de 2013). *Boletín de la Sociedad Argentina de Botánica* 49: 327–339.
- Sunesen I., Méndez S.M., Mancera-Pineda J.E., Dechraoui Bottein M.-Y. & Enevoldsen H. 2021. The Latin America and Caribbean HAB status report based on OBIS and HAEDAT maps and databases. *Harmful Algae* 102: Article 101920. DOI: [10.1016/j.hal.2020.101920](https://doi.org/10.1016/j.hal.2020.101920).

- Tamura K. & Nei M. 1993. Estimation of the number of nucleotide substitutions in the control region of mitochondrial DNA in humans and chimpanzees. *Molecular Biology and Evolution* 10: 512–526. DOI: [10.1093/oxfordjournals.molbev.a040023](https://doi.org/10.1093/oxfordjournals.molbev.a040023).
- Tardivo Kubis J.A., Lavigne A.S., Aguiar Juárez D., Risso A., Sar E.A. & Sunesen I. 2019. Monitoreo de microalgas nocivas y monitoreo de ficotoxinas en moluscos en la costa bonaerense. *Revista Estudios Ambientales* 6: 581–584. [In: *Resúmenes extendidos de las II Jornadas Internacionales y IV Nacionales de Ambiente "Integrando Ambiente, Comunidad y Compromiso"*, UNICEN, Tandil.]
- Tardivo Kubis J.A., Rodríguez F., Rossignoli A.E., Riobó P., Sar E.A. & Sunesen I. 2023. Morphological, phylogenetic and toxinological characterization of potentially harmful algal species from the marine coastal waters of Buenos Aires Province (Argentina). *Phycology* 3: 79–105. DOI: [10.3390/phycology3010006](https://doi.org/10.3390/phycology3010006).
- Tillman U., Bantle A., Krock B., Elbrächter M. & Gottschling M. 2021. Recommendations for epitypification of dinophytes exemplified by *Lingulodinium polyedra* and molecular phylogenetics of the Gonyaulacales based on curated rRNA sequence data. *Harmful Algae* 104: Article 101956. DOI: [10.1016/j.hal.2020.101956](https://doi.org/10.1016/j.hal.2020.101956).
- Touzet N., Franco J.M. & Raine R. 2008. Morphogenetic diversity and biotoxin composition of *Alexandrium* (Dinophyceae) in Irish coastal waters. *Harmful Algae* 7: 782–797. DOI: [10.1016/j.hal.2008.04.001](https://doi.org/10.1016/j.hal.2008.04.001).
- Usup G., Pin L.C., Ahmad A. & Teen L.P. 2002. *Alexandrium* (Dinophyceae) species in Malaysian waters. *Harmful Algae* 1: 265–275. DOI: [10.1016/S1568-9883\(02\)00044-6](https://doi.org/10.1016/S1568-9883(02)00044-6).
- Van de Waal D.B., Tillmann U., Martens H., Krock B., van Scheppingen Y. & John U. 2015. Characterization of multiple isolates from an *Alexandrium ostenfeldii* bloom in The Netherlands. *Harmful Algae* 29: 94–104. DOI: [10.1016/j.hal.2015.08.002](https://doi.org/10.1016/j.hal.2015.08.002).
- Varela D., Paredes J., Alves-de-Souza C., Seguel M., Sfeir A. & Frangópulos M. 2012. Intra-regional variation among *Alexandrium catenella* (Dinophyceae) strains from southern Chile: morphological, toxicological and genetic diversity. *Harmful Algae* 15: 8–18. DOI: [10.1016/j.hal.2011.10.029](https://doi.org/10.1016/j.hal.2011.10.029).
- Vera G., Fraga S., Franco J.M. & Sánchez G. 1999. Primer registro en el Perú del dinoflagelado *Alexandrium affine* Inoue & Fukuyo. *Informe Progresivo del Instituto del Mar del Perú* 15: 1–12.
- Wang D.-Z., Zhang S.-G., Gu H.-F., Chan L.L. & Hong H.-S. 2006. Paralytic shellfish toxin profiles and toxin variability of the genus *Alexandrium* (Dinophyceae) isolated from the Southeast China Sea. *Toxicon* 48: 138–151. DOI: [10.1016/j.toxicon.2006.04.002](https://doi.org/10.1016/j.toxicon.2006.04.002).
- Xu Y., He X., Li H., Zhang T., Lei F., Gu H. & Anderson D.M. 2021. Molecular identification and toxin analysis of *Alexandrium* spp. in the Beibu Gulf: first report of toxic *A. tamiyavanichii* in Chinese coastal waters. *Toxins* 13: Article 161. DOI: [10.3390/toxins13020161](https://doi.org/10.3390/toxins13020161).